# A finite element solution of acoustic propagation in rigid porous media

A. Bermúdez*, J. L. Ferrín* and A. Prieto*

**Abstract**

This paper deals with the acoustical behavior of a rigid porous material. A finite element method to compute both the response to an harmonic excitation and the free vibrations of a three-dimensional finite multilayer system consisting of a free fluid and a rigid porous material is considered. The finite element used is the lowest order face element introduced by Raviart and Thomas, that eliminates the spurious or circulation modes with no physical meaning. For the porous medium a Darcy's like model and the Allard-Champoux model are taken into account. The numerical results show that the finite element method allows us to compute the response curve for the coupled system and the complex eigenfrequencies. Some of them have a small imaginary part but there are also overdamped modes.

**Keywords:** Rigid frame; Porous medium; Finite element method

## 1 INTRODUCTION

Porous materials are widely used in several noise control applications. These materials are known for their ability to dissipate acoustic waves propagating along them. Extensive work has been done to characterize the acoustical behavior of such materials. By porous material we mean a material consisting of a solid matrix which is completely saturated by a fluid. The acoustical behavior of the porous medium depends not only on the fluid but also on the rigidity of the skeleton.

In the past, simplified models where absorptive materials are characterized by normal wave impedance have been used to study wave propagation in rigid lined ducted systems. More recently, when the solid skeleton is rigid the porous material has been considered as an equivalent fluid with equivalent density and bulk modulus. These parameters can be obtained through empirical or experimental laws. A first model by Delany and Bazley [16] was presented for the first time in 1970; it has been widely used to describe sound propagation in fibrous materials. Subsequently, this model was improved in works by Morse and Ingard [25], Johnson *et al* [22], Attenborough [6], Allard *et al* [4], Champoux and Stinson [14] or Allard and Champoux [3], among others.

For the more realistic case when the elastic deformation of the skeleton is taken into account, the theoretical basis for the mechanical behavior was mainly established by Biot [11]. His theory describes the propagation of elastic waves in fluid-saturated porous media. Adaption of this theory to acoustics was made, for example, in works by Allard *et al* [2] and Shiau [29] (see also in the complete reference by Allard [1]).

Another way to derive models simulating a slow fluid flow through porous media, rigorously from a mathematical point of view, is by using the theory of homogenization. When a rigid porous medium is considered, the model obtained is named Darcy's model. Ene and Sanchez-Palencia [18] seem to be the first to give a derivation of it from the Stokes system using a formal multiscale method. This derivation was made rigorous in the case of 2D periodic rigid porous media by Tartar (see appendix in [28]) and subsequently generalized among others by Mikelić (see [24] and references therein). This methodology allows us not only to obtain the homogenized model but also the mathematical expression of the coefficients appearing in it. For instance, in the case of rigid porous media, the most important coefficient in Darcy's law is permeability, which can be computed by solving a boundary-value problem in a unit cell of the periodic

*Departamento de Matemática Aplicada, Universidad de Santiago de Compostela, 15782 Santiago de Compostela, Spain.

porous medium. For poroelastic media, generalized Biot models were also derived from the first principles by using homogenization techniques (see Gilbert and Mikelić [20], by Clopeau *et al* [15] or Ferrín and Mikelić [19]).

Concerning the numerical solution of both cases, the rigid and the elastic solid skeleton, an increasing number of papers can be found. Because of its easy implementation and its effectiveness in handling complex geometries, the finite element method has become popular to solve such problems. Some examples of the finite element method applied to sound propagation in poroelastic media are papers by Easwaran *et al* [17], Panneton and Atalla [26], Göransson [21] or Atalla *et al* [5]. All of them, take Biot's general theory as the starting point. Other kind of problems concerning porous materials, related to vibration modes, were solved by Bermúdez *et al* [9].

In this paper, only the case of rigid frame porous material will be considered. Two models will be taken into account: the above mentioned sort of Darcy's model and the Allard-Champoux model (see Allard and Champoux [3]). The main difference between them lies in the frequency dependence of the coefficients, namely, density and stiffness. A finite element method introduced by Raviart and Thomas [27] will be used to solve numerically the two models which are formulated in displacements. It has been proven in Bermúdez *et al* [10] (see also [8] and references therein) that these finite elements do not produce spurious modes. In the Allard-Champoux model both the mass and the stiffness matrices are frequency-dependent, forcing us to calculate them for each frequency. Numerical experiments using both models will be presented over different three-dimensional examples. More precisely, we solve the source problem associated with an external harmonic excitation which allows us to know the response of the porous material. We also solve the nonlinear spectral problem associated with it.

The outline of this paper is as follows. In section 2 we present the two models associated with the problem consisting of a finite two-layer system with rigid porous materials. They will be stated in the frequency domain leading to the response problem and to a nonlinear eigenvalue problem. In section 3 the free vibration problem associated with a nonlinear eigenvalue problem is analyzed in order to obtain a deeper insight of the overdamped vibration frequencies. In section 4 the weak formulations for both problems are presented and an analysis of overdamped vibration frequencies is made. In section 5 the finite element method is introduced, whereas in section 6 the corresponding matricial description is shown. Finally, in section 7, numerical results for some 3D examples are given for both the response and the spectral problems.

# 2 MODELS FOR FLUID-POROUS VIBRATIONS

Let us consider a coupled system consisting of an acoustic fluid (i.e. compressible barotropic inviscid) and a porous medium contained in a three-dimensional cavity. Let $\Omega_{\mathrm{F}}$ and $\Omega_{\mathrm{A}}$ be the domains occupied by the fluid and the porous medium, respectively (see figure 1). The boundary of $\overline{\Omega}_{\mathrm{F}} \cup \overline{\Omega}_{\mathrm{A}}$, denoted by $\Gamma$, is the union of two parts, $\Gamma_{\mathrm{D}}$ and $\Gamma_{\mathrm{N}}$. $\Gamma_{\mathrm{D}}$ denotes the rigid walls of the cavity. Let $\boldsymbol{\nu}$ the outward unit normal vector to $\Gamma$. We assume the interface between the fluid and the porous media, denoted by $\Gamma_{\mathrm{I}}$, is the union of surfaces, $\Gamma_0, \Gamma_1, \dots, \Gamma_J$. Let $\mathbf{n}$ be the unit normal vector to this interface pointing outwards $\Omega_{\mathrm{A}}$. Figure 1 shows a vertical cut of the domain for a better understanding of the notation.

For studying the response of the coupled system (fluid-porous medium), subject to harmonic forces acting on $\Gamma_{\mathrm{N}}$, we consider two different models for the vibrations in the porous medium: Darcy's like model and Allard-Champoux model. Both models assume the skeleton of the porous media is rigid.

Firstly, the governing equations for free small amplitude motions of an acoustic fluid filling $\Omega_{\mathrm{F}}$ are given in terms of displacement and pressure fields by

$$\rho_{\mathrm{F}} \frac{\partial^2 \mathbf{U}_{\mathrm{F}}}{\partial t^2} + \operatorname{grad} P_{\mathrm{F}} = \mathbf{0} \quad \text{in} \quad \Omega_{\mathrm{F}}, \tag{1}$$

$$P_{\mathrm{F}} = -\rho_{\mathrm{F}} c^2 \operatorname{div} \mathbf{U}_{\mathrm{F}} \quad \text{in} \quad \Omega_{\mathrm{F}}, \tag{2}$$

where $P_{\mathrm{F}}$ is the pressure, $\mathbf{U}_{\mathrm{F}}$ the displacement field, $\rho_{\mathrm{F}}$ the density and $c$ the acoustic speed in the fluid.

Moreover, in the porous medium, the Darcy's like model only has slight differences with the above fluid model. One of them consists of an additional damping term, named Darcy's term (see [1]). Moreover, the interstitial fluid flow is supposed to be isothermal, a standard assumption in porous media acoustics. If $\mathbf{U}_{\mathrm{A}}$

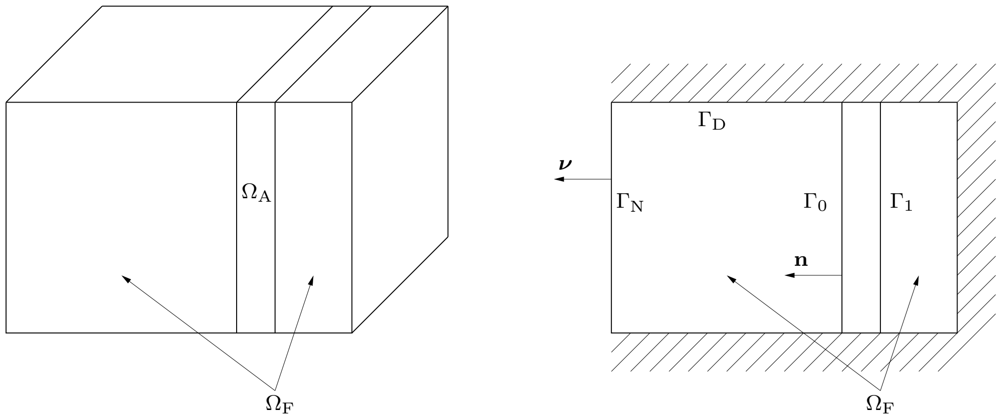


Figure 1: 3D domain and vertical cut.

is the displacement field and $P_A$ is the pressure in the porous medium, the Darcy's like model is described by the following equations,

$$\rho_F \frac{\partial^2 \mathbf{U}_A}{\partial t^2} + \text{grad } P_A + \boldsymbol{\sigma} \frac{\partial \mathbf{U}_A}{\partial t} = \mathbf{0} \quad \text{in} \quad \Omega_A, \tag{3}$$

$$P_A = -\frac{\rho_F c^2}{\phi \gamma} \text{div } \mathbf{U}_A \quad \text{in} \quad \Omega_A, \tag{4}$$

where $\boldsymbol{\sigma}$ is the flow resistivity tensor, $\phi$ is the porosity, $\gamma$ is the ratio of specific heats of fluid and, again, $\rho_F$ is the density and $c$ the acoustic speed of the fluid filling the porous medium. The flow resistivity $\boldsymbol{\sigma}$ is related to the permeability tensor through $\boldsymbol{\sigma} = \mu\phi\mathbf{R}^{-1}$, where $\mu$ is the viscosity coefficient of the fluid. For periodic porous media, the permeability tensor can be obtained using homogenization methods by solving partial differential equations in the unit cell (see Tartar[28] or Mikelić [24]).

Since we neglect viscosity in the fluid and shear stresses in the porous media, only the normal component of the displacement vanishes on the part $\Gamma_D$ of the cavity boundary,

$$\mathbf{U}_F \cdot \boldsymbol{\nu} = 0 \quad \text{on} \quad \Gamma_D \cap \partial\Omega_F, \tag{5}$$

$$\mathbf{U}_A \cdot \boldsymbol{\nu} = 0 \quad \text{on} \quad \Gamma_D \cap \partial\Omega_A. \tag{6}$$

Similarly, on the interface $\Gamma_I$ between the fluid and the porous medium we consider the usual kinematic and kinetic interface conditions, i.e., $\mathbf{U}_F \cdot \mathbf{n} = \mathbf{U}_A \cdot \mathbf{n}$ and $P_F = P_A$.

If a displacement $F$ is applied on $\Gamma_N$, the equations describing the motion of the coupled system can be written, when we use the above model, as follows (see [1]):

$$\rho_F \frac{\partial^2 \mathbf{U}_F}{\partial t^2} + \text{grad } P_F = \mathbf{0} \quad \text{in} \quad \Omega_F, \tag{7}$$

$$\rho_F \frac{\partial^2 \mathbf{U}_A}{\partial t^2} + \text{grad } P_A + \boldsymbol{\sigma} \frac{\partial \mathbf{U}_A}{\partial t} = \mathbf{0} \quad \text{in} \quad \Omega_A, \tag{8}$$

$$P_F = -\rho_F c^2 \text{div } \mathbf{U}_F \quad \text{in} \quad \Omega_F, \tag{9}$$

$$P_A = -\frac{\rho_F c^2}{\phi \gamma} \text{div } \mathbf{U}_A \quad \text{in} \quad \Omega_A, \tag{10}$$

$$P_F = P_A \quad \text{on} \quad \Gamma_I, \tag{11}$$

$$\mathbf{U}_F \cdot \mathbf{n} = \mathbf{U}_A \cdot \mathbf{n} \quad \text{on} \quad \Gamma_I, \tag{12}$$

$$\mathbf{U}_F \cdot \boldsymbol{\nu} = 0 \quad \text{on} \quad \Gamma_D \cap \partial\Omega_F, \tag{13}$$

$$\mathbf{U}_A \cdot \boldsymbol{\nu} = 0 \quad \text{on} \quad \Gamma_D \cap \partial\Omega_A, \tag{14}$$

$$\mathbf{U}_F \cdot \boldsymbol{\nu} = F \quad \text{on} \quad \Gamma_N. \tag{15}$$

We are interested in harmonic vibrations. Thus, we suppose the displacement is of the form,

$$F(x,y,z,t)=\mathrm{Re}\left(e^{i\omega t}f(x,y,z)\right). \tag{16}$$

Then, all fields are harmonic, i.e.,

$$\begin{aligned}
\mathbf{U}_{\mathrm{F}}(x,y,z,t) &= \mathrm{Re}\left(e^{i\omega t}\mathbf{u}_{\mathrm{F}}(x,y,z)\right), &(17)\\
\mathbf{U}_{\mathrm{A}}(x,y,z,t) &= \mathrm{Re}\left(e^{i\omega t}\mathbf{u}_{\mathrm{A}}(x,y,z)\right), &(18)\\
P_{\mathrm{F}}(x,y,z,t) &= \mathrm{Re}\left(e^{i\omega t}p_{\mathrm{F}}(x,y,z)\right), &(19)\\
P_{\mathrm{A}}(x,y,z,t) &= \mathrm{Re}\left(e^{i\omega t}p_{\mathrm{A}}(x,y,z)\right). &(20)
\end{aligned}$$

By replacing these expressions into the above equations, we can define an harmonic source problem associated with the evolutionary source problem (7)-(15), namely,

$$\begin{aligned}
-\omega^2\rho_{\mathrm{F}}\mathbf{u}_{\mathrm{F}}+\mathrm{grad}\ p_{\mathrm{F}}=\mathbf{0} &\quad \text{in} \quad \Omega_{\mathrm{F}}, &(21)\\
-\omega^2\rho_{\mathrm{F}}\left(1+\frac{\boldsymbol{\sigma}}{i\omega\rho_{\mathrm{F}}}\right)\mathbf{u}_{\mathrm{A}}+\mathrm{grad}\ p_{\mathrm{A}}=\mathbf{0} &\quad \text{in} \quad \Omega_{\mathrm{A}}, &(22)\\
p_{\mathrm{F}}=-\rho_{\mathrm{F}}c^2\mathrm{div}\ \mathbf{u}_{\mathrm{F}} &\quad \text{in} \quad \Omega_{\mathrm{F}}, &(23)\\
p_{\mathrm{A}}=-\frac{\rho_{\mathrm{F}}c^2}{\phi\gamma}\mathrm{div}\ \mathbf{u}_{\mathrm{A}} &\quad \text{in} \quad \Omega_{\mathrm{A}}, &(24)\\
p_{\mathrm{F}}=p_{\mathrm{A}} &\quad \text{on} \quad \Gamma_{\mathrm{I}}, &(25)\\
\mathbf{u}_{\mathrm{F}}\cdot\mathbf{n}=\mathbf{u}_{\mathrm{A}}\cdot\mathbf{n} &\quad \text{on} \quad \Gamma_{\mathrm{I}}, &(26)\\
\mathbf{u}_{\mathrm{F}}\cdot\boldsymbol{\nu}=0 &\quad \text{on} \quad \Gamma_{\mathrm{D}}\cap\partial\Omega_{\mathrm{F}}, &(27)\\
\mathbf{u}_{\mathrm{A}}\cdot\boldsymbol{\nu}=0 &\quad \text{on} \quad \Gamma_{\mathrm{D}}\cap\partial\Omega_{\mathrm{A}}, &(28)\\
\mathbf{u}_{\mathrm{F}}\cdot\boldsymbol{\nu}=f &\quad \text{on} \quad \Gamma_{\mathrm{N}}. &(29)
\end{aligned}$$

In this context, looking for harmonic motions, we can also consider the Allard-Champoux model (see [3]) for rigid frame fibrous materials (a particular case of porous medium with rigid solid part). In this case, not only the Darcy's term is included in a new generalized form but also the thermal exchange between the air and the fibers of the porous medium is considered in the model. The new equations replacing (22) and (24) are

$$\begin{aligned}
-\omega^2\boldsymbol{\rho}(\omega)\mathbf{u}_{\mathrm{A}}+\mathrm{grad}\ p_{\mathrm{A}}=\mathbf{0} &\quad \text{in} \quad \Omega_{\mathrm{A}}, &(30)\\
p_{\mathrm{A}}=-\mathrm{div}\left(\mathbf{K}(\omega)\mathbf{u}_{\mathrm{A}}\right) &\quad \text{in} \quad \Omega_{\mathrm{A}}, &(31)
\end{aligned}$$

where $\boldsymbol{\rho}(\omega)$ and $\mathbf{K}(\omega)$ are the so called dynamic density tensor and dynamic bulk modulus tensor, respectively. If the porous medium is isotropic these tensors are multiple of the identity, i.e. $\mathbf{K}(\omega)=K(\omega)\mathbf{I},\ \boldsymbol{\rho}(\omega)=\rho(\omega)\mathbf{I}$, where (see [3]),

$$\begin{aligned}
\rho(\omega) &= \rho_{\mathrm{F}}\left(1-i\left(\frac{\sigma}{\rho_{\mathrm{F}}\omega}\right)G_1\left(\frac{\rho_{\mathrm{F}}\omega}{\sigma}\right)\right), &(32)\\
K(\omega) &= \gamma P_0\left(\gamma-\frac{\gamma-1}{1-(\frac{i}{4N_{pr}})(\frac{\sigma}{\rho_{\mathrm{F}}\omega})G_2(\frac{\rho_{\mathrm{F}}\omega}{\sigma})}\right)^{-1}. &(33)
\end{aligned}$$

In the above empirical equations $P_0$ is the fluid equilibrium pressure, $\gamma$ is the ratio of specific heats of fluid, $N_{pr}$ is the Prandtl number and $\sigma$ is the flow resistivity. Finally, functions $G_1$ and $G_2$ are given by

$$\begin{aligned}
G_1\left(\frac{\rho_{\mathrm{F}}\omega}{\sigma}\right) &= \sqrt{1+\frac{i}{2}\left(\frac{\rho_{\mathrm{F}}\omega}{\sigma}\right)}, &(34)\\
G_2\left(\frac{\rho_{\mathrm{F}}\omega}{\sigma}\right) &= G_1\left(4N_{pr}\left(\frac{\rho_{\mathrm{F}}\omega}{\sigma}\right)\right). &(35)
\end{aligned}$$

Because of the expressions of $G_1$ and $G_2$, both the dynamic density and the bulk modulus are functions of the quotient $\frac{\rho_{\rm F}\omega}{\sigma}$. Then, if we assume that $\rho_{\rm F}\omega \ll \sigma$, by neglecting the terms involving $\left(\frac{\rho_{\rm F}\omega}{\sigma}\right)^2$, we obtain the following approximations

$$\rho(\omega) \simeq \rho_{\rm F} + \frac{\sigma}{i\omega} \text{ and } K(\omega) \simeq P_0 \simeq \frac{\rho_{\rm F} c^2}{\phi\gamma}, \tag{36}$$

which show that the Darcy's like model and Allard-Champoux model are equivalent for low frequencies when the porosity is nearly unity.

Drawing an analogy with the harmonic source problem (21)-(29), we can establish a similar one using the Allard-Champoux model (30)-(35):

$$\begin{aligned}
-\omega^2\rho_{\rm F}\mathbf{u}_{\rm F} + \text{grad}\, p_{\rm F} = \mathbf{0} &\quad \text{in} \quad \Omega_{\rm F}, &(37)\\
-\omega^2\boldsymbol{\rho}(\omega)\mathbf{u}_{\rm A} + \text{grad}\, p_{\rm A} = \mathbf{0} &\quad \text{in} \quad \Omega_{\rm A}, &(38)\\
p_{\rm F} = -\rho_{\rm F} c^2 \text{div}\, \mathbf{u}_{\rm F} &\quad \text{in} \quad \Omega_{\rm F}, &(39)\\
p_{\rm A} = -\text{div}\,(\mathbf{K}(\omega)\mathbf{u}_{\rm A}) &\quad \text{in} \quad \Omega_{\rm A}, &(40)\\
p_{\rm F} = p_{\rm A} &\quad \text{on} \quad \Gamma_{\rm I}, &(41)\\
\mathbf{u}_{\rm F}\cdot\mathbf{n} = \mathbf{u}_{\rm A}\cdot\mathbf{n} &\quad \text{on} \quad \Gamma_{\rm I}, &(42)\\
\mathbf{u}_{\rm F}\cdot\boldsymbol{\nu} = 0 &\quad \text{on} \quad \Gamma_{\rm D}\cap\partial\Omega_{\rm F}, &(43)\\
\mathbf{u}_{\rm A}\cdot\boldsymbol{\nu} = 0 &\quad \text{on} \quad \Gamma_{\rm D}\cap\partial\Omega_{\rm A}, &(44)\\
\mathbf{u}_{\rm F}\cdot\boldsymbol{\nu} = f &\quad \text{on} \quad \Gamma_{\rm N}. &(45)
\end{aligned}$$

# 3 ASSOCIATED NONLINEAR EIGENVALUE PROBLEMS

We can define a nonlinear eigenvalue problem, associated with the above source problem (37)-(45), which corresponds to determining the free vibrations of the fluid-porous system. More precisely, if we assume that $f = 0$ in the system (37)-(45), we can define the following problem:

*Find a complex angular frequency $\omega$ and complex amplitudes of pressure and displacement fields $(p_F, p_A)$ and $(\mathbf{u}_F, \mathbf{u}_A)$, respectively, not all identically zero, satisfying*

$$\begin{aligned}
-\omega^2\rho_{\rm F}\mathbf{u}_{\rm F} + \text{grad}\, p_{\rm F} = \mathbf{0} &\quad \text{in} \quad \Omega_{\rm F}, &(46)\\
-\omega^2\boldsymbol{\rho}(\omega)\mathbf{u}_{\rm A} + \text{grad}\, p_{\rm A} = \mathbf{0} &\quad \text{in} \quad \Omega_{\rm A}, &(47)\\
p_{\rm F} = -\rho_{\rm F} c^2 \text{div}\, \mathbf{u}_{\rm F} &\quad \text{in} \quad \Omega_{\rm F}, &(48)\\
p_{\rm A} = -\text{div}\,(\mathbf{K}(\omega)\mathbf{u}_{\rm A}) &\quad \text{in} \quad \Omega_{\rm A}, &(49)\\
p_{\rm F} = p_{\rm A} &\quad \text{on} \quad \Gamma_{\rm I}, &(50)\\
\mathbf{u}_{\rm F}\cdot\mathbf{n} = \mathbf{u}_{\rm A}\cdot\mathbf{n} &\quad \text{on} \quad \Gamma_{\rm I}, &(51)\\
\mathbf{u}_{\rm F}\cdot\boldsymbol{\nu} = 0 &\quad \text{on} \quad \Gamma\cap\partial\Omega_{\rm F}, &(52)\\
\mathbf{u}_{\rm A}\cdot\boldsymbol{\nu} = 0 &\quad \text{on} \quad \Gamma\cap\partial\Omega_{\rm A}. &(53)
\end{aligned}$$

On the other hand, if we used the Darcy's like model (7)-(15), we still obtain the above eigenvalue problem but the expressions for the dynamic density and the bulk modulus change. In this case, they are $\boldsymbol{\rho}(\omega) = \rho_{\rm F}\mathbf{I} + \frac{\boldsymbol{\sigma}}{i\omega}$ and $\mathbf{K}(\omega) = \frac{\rho_{\rm F} c^2}{\phi\gamma}\mathbf{I}$.

The solutions $\omega$ of this nonlinear eigenvalue problem (46)-(53) are expected to be complex numbers with non-null real and imaginary parts due to the dissipative terms. The real part corresponds to the angular frequency of the damped vibration mode, whereas the imaginary part corresponds to its decay rate and should be strictly positive. However, as the example below shows, overdamped modes corresponding to purely imaginary positive values of $\omega$ also exist.

To gain a deeper insight into these overdamped modes, let us introduce a simpler model problem for which these eigenvalues can be computed analytically. Let us take $\Omega_{\rm F} = (-a_{\rm F}, 0)\times(0,b)\times(0,d)$, $\Omega_{\rm A} =$

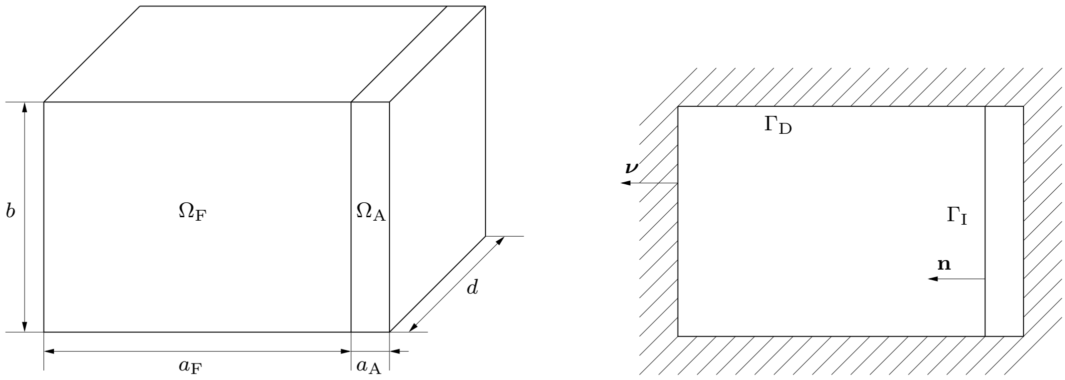


Figure 2: Fluid and rigid porous medium in a cavity with rigid walls.

$(0, a_\mathrm{A}) \times (0, b) \times (0, d)$, $\Gamma_\mathrm{D} = \Gamma$ and $\Gamma_\mathrm{N} = \emptyset$ (see figure 2). If we consider the Darcy's like model, the eigenvalue problem can be solved by separation of variables.

For this purpose, it is convenient to write the problem in terms of pressure. This can be done by eliminating $\mathbf{u}_\mathrm{F}$ and $\mathbf{u}_\mathrm{A}$ in equations (46)-(47) by using (48) and (49). Thus we obtain:

$$\omega^2 p_\mathrm{F} + c^2 \Delta p_\mathrm{F} = 0 \quad \text{in} \quad \Omega_\mathrm{F}, \tag{54}$$

$$\omega^2 \left(1 + \frac{\sigma}{i\omega\rho_\mathrm{F}}\right) p_\mathrm{A} + \frac{c^2}{\phi\gamma} \Delta p_\mathrm{A} = 0 \quad \text{in} \quad \Omega_\mathrm{A}, \tag{55}$$

$$p_\mathrm{F} = p_\mathrm{A} \quad \text{on} \quad \Gamma_\mathrm{I}, \tag{56}$$

$$\frac{1}{\rho_\mathrm{F}} \frac{\partial p_\mathrm{F}}{\partial \mathbf{n}} = \frac{1}{\rho_\mathrm{F} + \frac{\sigma}{i\omega}} \frac{\partial p_\mathrm{A}}{\partial \mathbf{n}} \quad \text{on} \quad \Gamma_\mathrm{I}, \tag{57}$$

$$\frac{\partial p_\mathrm{F}}{\partial \boldsymbol{\nu}} = 0 \quad \text{on} \quad \Gamma_\mathrm{D} \cap \partial\Omega_\mathrm{F}, \tag{58}$$

$$\frac{\partial p_\mathrm{A}}{\partial \boldsymbol{\nu}} = 0 \quad \text{on} \quad \Gamma_\mathrm{D} \cap \partial\Omega_\mathrm{A}. \tag{59}$$

If we look for non-trivial solutions of this problem of the form

$$p_\mathrm{F}(x, y, z) = X_\mathrm{F}(x) Y_\mathrm{F}(y) Z_\mathrm{F}(z),$$
$$p_\mathrm{A}(x, y, z) = X_\mathrm{A}(x) Y_\mathrm{A}(y) Z_\mathrm{A}(z),$$

standard calculations show that:

$$Y_\mathrm{F}(y) = \cos \frac{j\pi y}{b}, \; Y_\mathrm{A}(y) = \cos \frac{j\pi y}{b}, \; j = 0, \pm 1, \pm 2, \dots \tag{60}$$

$$Z_\mathrm{F}(z) = \cos \frac{k\pi z}{d}, \; Z_\mathrm{A}(z) = \cos \frac{k\pi z}{d}, \; k = 0, \pm 1, \pm 2, \dots \tag{61}$$

Furthermore, for any pair of integers $j$ and $k$, we must have

$$X_\mathrm{F}'' = \mu_\mathrm{F}^2 X_\mathrm{F}, \; -a_\mathrm{F} < x < 0, \tag{62}$$

$$X_\mathrm{A}'' = \mu_\mathrm{A}^2 X_\mathrm{A}, \; 0 < x < a_\mathrm{A}, \tag{63}$$

$$X_\mathrm{F}(0) = X_\mathrm{A}(0), \tag{64}$$

$$\frac{1}{\rho_\mathrm{F}} X_\mathrm{F}'(0) = \frac{1}{\rho_\mathrm{F} + \frac{\sigma}{i\omega}} X_\mathrm{A}'(0), \tag{65}$$

$$X_\mathrm{F}'(-a_\mathrm{F}) = 0, \tag{66}$$

$$X_\mathrm{F}'(a_\mathrm{A}) = 0, \tag{67}$$

with

$$\mu_{\mathrm{F}}^2 + \frac{\omega^2}{c^2} = \frac{\pi^2}{b^2} j^2 + \frac{\pi^2}{d^2} k^2, \tag{68}$$

$$\mu_{\mathrm{A}}^2 + \omega^2 \frac{\phi\gamma}{c^2} \left(1 + \frac{\sigma}{i\rho_{\mathrm{F}}\omega}\right) = \frac{\pi^2}{b^2} j^2 + \frac{\pi^2}{d^2} k^2. \tag{69}$$

The general solutions of (62) and (63) are $X_{\mathrm{F}}(x) = C_{\mathrm{F},1} e^{\mu_{\mathrm{F}} x} + C_{\mathrm{F},2} e^{-\mu_{\mathrm{F}} x}$ and $X_{\mathrm{A}}(x) = C_{\mathrm{A},1} e^{\mu_{\mathrm{A}} x} + C_{\mathrm{A},2} e^{-\mu_{\mathrm{A}} x}$. By replacing these expressions in (64)-(67) and after some calculations, we obtain the following dispersion relation:

$$\mu_{\mathrm{F}} \left(\rho_{\mathrm{F}} + \frac{\sigma}{i\omega}\right) \cosh(a_{\mathrm{A}}\mu_{\mathrm{A}}) \sinh(a_{\mathrm{F}}\mu_{\mathrm{F}}) + \mu_{\mathrm{A}}\rho_{\mathrm{F}} \sinh(a_{\mathrm{A}}\mu_{\mathrm{A}}) \cosh(a_{\mathrm{F}}\mu_{\mathrm{F}}) = 0. \tag{70}$$

For any pair of integers $j$ and $k$, this equation together with (68) and (69) constitute a nonlinear system which has complex solutions $(\omega, \mu_{\mathrm{F}}) \in \mathbb{C}^2$ if we consider $\mu_{\mathrm{A}}$ as an expression that depends on $\omega$ and $\mu_{\mathrm{F}}$ via

$$\mu_A = \sqrt{\mu_{\mathrm{F}}^2 + \frac{i\omega}{c^2} \frac{\phi\gamma\sigma}{\rho} - \frac{\omega^2}{c^2}(1 - \phi\gamma)}, \tag{71}$$

which is obtained from (68) and (69).

As we show below, for some of these solutions $\omega$ is a purely imaginary positive number. To see this, we plot in figures 3 and 4 the curves obtained from equations (68)-(70) for positive real values of $\mu_{\mathrm{F}}$ and $\lambda = -i\omega$ (i.e., purely imaginary positive values of $\omega = i\lambda$).

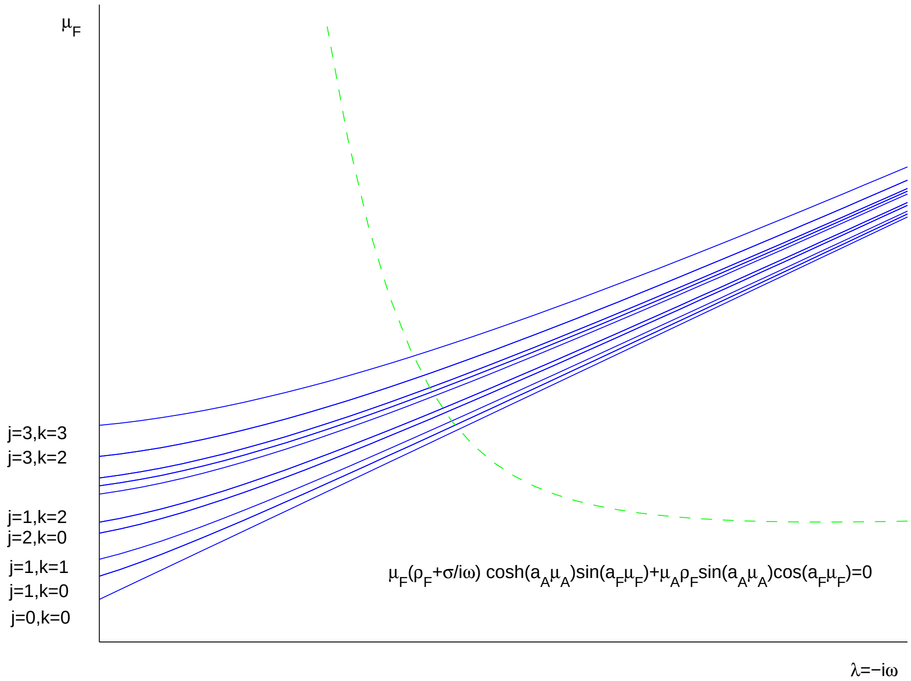


Figure 3: Curves (68) and (70) for real values of $\mu_{\mathrm{F}}$ and $\lambda = -i\omega$; case $a_{\mathrm{A}} < \pi\frac{\rho c}{\sigma}$.

If we assume that $a_{\mathrm{F}} > a_{\mathrm{A}}$, it can be seen that the resulting curves intersect differently in case of $a_{\mathrm{A}} < \pi\frac{\rho_{\mathrm{F}} c}{\sigma}\sqrt{\frac{1}{3-\phi\gamma}}$ or $a_{\mathrm{A}} > \pi\frac{\rho_{\mathrm{F}} c}{\sigma}\sqrt{\frac{1}{3-\phi\gamma}}$. More precisely, the following alternative holds:

- If $a_{\mathrm{A}} < \pi\frac{\rho_{\mathrm{F}} c}{\sigma}\sqrt{\frac{1}{3-\phi\gamma}}$, then for any pair of integers $j, k = 0, 1, 2, \ldots$, there exists a solution $(\omega_{jk}, \mu_{\mathrm{F},jk})$ of (68)-(70), with $\omega_{jk} = i\lambda_{jk}$ satisfying

$$\frac{\sigma}{2\rho_{\mathrm{F}}} < \lambda_{jk} \leq \max\left\{\frac{\sigma}{\rho_{\mathrm{F}}}, \frac{\sigma}{\rho_{\mathrm{F}}\phi\gamma}\right\} \text{ and } \lambda_{jk} \to \frac{\sigma}{2\rho_{\mathrm{F}}} \text{ as } \frac{j^2}{b^2} + \frac{k^2}{d^2} \to \infty. \tag{72}$$

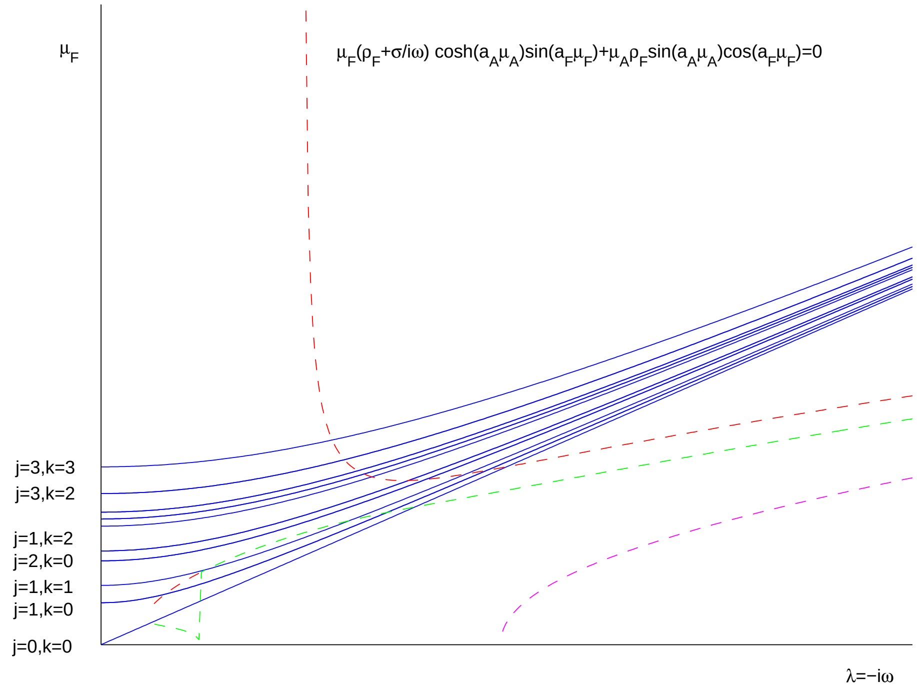


Figure 4: Curves (68) and (70) for real values of $\mu_{\mathrm{F}}$ and $\lambda = -i\omega$; case $a_{\mathrm{A}} > \pi\frac{\rho c}{\sigma}$.

- If $a_{\mathrm{A}} > \pi\frac{\rho_{\mathrm{F}} c}{\sigma}\sqrt{\frac{1}{3-\phi\gamma}}$, then for any pair of integers $j, k = 0, 1, 2, \ldots$, there exists a solution $(\omega_{jk}, \mu_{\mathrm{F},jk})$ of (68)-(70), with $\omega_{jk} = i\lambda_{jk}$ satisfying

$$0 < \lambda_{jk} \le \max\left\{\frac{\sigma}{\rho_{\mathrm{F}}}, \frac{\sigma}{\rho_{\mathrm{F}}\phi\gamma}\right\} \text{ and } \lambda_{jk} \to \frac{\sigma}{2\rho_{\mathrm{F}}} \text{ as } \frac{j^2}{b^2} + \frac{k^2}{d^2} \to \infty. \tag{73}$$

Each of these solutions $(\omega_{jk}, \mu_{\mathrm{F},jk})$ yields an eigenmode of (54)-(59) with

$$p_{\mathrm{F},jk}(x,y,z) = \cos\frac{j\pi y}{a}\cos\frac{k\pi z}{d}\left(C_{\mathrm{F},1}e^{\mu_{\mathrm{F},jk}x} + C_{\mathrm{F},2}e^{-\mu_{\mathrm{F},jk}x}\right), \ -a_{\mathrm{F}} < x < 0, \tag{74}$$

$$p_{\mathrm{A},jk}(x,y,z) = \cos\frac{j\pi y}{a}\cos\frac{k\pi z}{d}\left(C_{\mathrm{A},1}e^{\mu_{\mathrm{A},jk}x} + C_{\mathrm{A},2}e^{-\mu_{\mathrm{A},jk}x}\right), \ 0 < x < a_{\mathrm{A}}, \tag{75}$$

where

$$\mu_{\mathrm{A},jk} = \sqrt{\mu_{\mathrm{F},jk}^2 - \frac{\lambda_{jk}}{c^2}\frac{\phi\gamma\sigma}{\rho} + \frac{\lambda_{jk}^2}{c^2}(\phi\gamma - 1)}. \tag{76}$$

For real porous-fluid configuration, the thickness of porous layer typically satisfies $a_{\mathrm{A}} < \pi\frac{\rho_{\mathrm{F}} c}{\sigma}\sqrt{\frac{1}{3-\phi\gamma}}$ and, in this case, the overdamped eigenvalues are always between $\frac{\sigma}{2\rho_{\mathrm{F}}}$ and $\frac{\sigma}{\rho_{\mathrm{F}}}$.

# 4 STATEMENT OF THE WEAK FORMULATION

For the sake of simplicity, we restrict our attention to the case where the porous medium is isotropic. Let us define the set $\mathbf{V}$ of kinematically admissible virtual displacements,

$$\mathbf{V} = \left\{(\mathbf{v}_{\mathrm{F}}, \mathbf{v}_{\mathrm{A}}) \in \mathbf{H} : \mathbf{v}_{\mathrm{F}} \cdot \mathbf{n} = \mathbf{v}_{\mathrm{A}} \cdot \mathbf{n} \text{ on } \Gamma_{\mathrm{I}}\right\},$$

where

$$\mathbf{H} = \{(\mathbf{v}_{\mathrm{F}}, \mathbf{v}_{\mathrm{A}}) \in \mathrm{H}(\mathrm{div}, \Omega_{\mathrm{F}}) \times \mathrm{H}(\mathrm{div}, \Omega_{\mathrm{A}}) \ : \ \mathbf{v}_{\mathrm{F}} \cdot \boldsymbol{\nu} = 0 \text{ on } \Gamma \cap \partial\Omega_{\mathrm{F}} \ , \qquad \mathbf{v}_{\mathrm{A}} \cdot \boldsymbol{\nu} = 0 \text{ on } \Gamma \cap \partial\Omega_{\mathrm{A}} \} \, ,$$

and

$$\mathrm{H}(\mathrm{div}, \Omega) = \left\{ \mathbf{v} \in (\mathrm{L}^2(\Omega))^3 : \ \mathrm{div}\ \mathbf{v} \in \mathrm{L}^2(\Omega) \right\} , \tag{77}$$

where $\mathrm{L}^2(\Omega)$ denotes the space of square integrable functions. To get a weak formulation of the eigenvalue problem (46)-(53), equation (46) is multiplied by the conjugate of a virtual fluid displacement $\bar{\mathbf{v}}_{\mathrm{F}}$ satisfying the Dirichlet condition (52) and then integrated in $\Omega_{\mathrm{F}}$. By using a Green's formula integration by parts and equation (48), we obtain

$$\int_{\Omega_{\mathrm{F}}} \rho_{\mathrm{F}} c^2 \mathrm{div}\ \mathbf{u}_{\mathrm{F}}\ \mathrm{div}\ \bar{\mathbf{v}}_{\mathrm{F}} - \int_{\Gamma_{\mathrm{I}}} p_{\mathrm{F}} \bar{\mathbf{v}}_{\mathrm{F}} \cdot \mathbf{n} = \omega^2 \int_{\Omega_{\mathrm{F}}} \rho_{\mathrm{F}} \mathbf{u}_{\mathrm{F}} \cdot \bar{\mathbf{v}}_{\mathrm{F}}. \tag{78}$$

In an analogous way, equations (47), (49) and (53) yield

$$\int_{\Omega_{\mathrm{A}}} K(\omega) \mathrm{div}\ \mathbf{u}_{\mathrm{A}}\ \mathrm{div}\ \bar{\mathbf{v}}_{\mathrm{A}} + \int_{\Gamma_{\mathrm{I}}} p_{\mathrm{A}} \bar{\mathbf{v}}_{\mathrm{A}} \cdot \mathbf{n} = \omega^2 \int_{\Omega_{\mathrm{A}}} \rho(\omega) \mathbf{u}_{\mathrm{A}} \cdot \bar{\mathbf{v}}_{\mathrm{A}}. \tag{79}$$

Now, by adding both equations and using the kinetic constraint (51), we can write the following pure displacement eigenvalue problem:

*Find a complex angular frequency* $\omega$ *and a pair of displacements* $(\mathbf{u}_{\mathrm{F}}, \mathbf{u}_{\mathrm{A}}) \in \mathbf{V}$, *with* $\mathbf{u}_{\mathrm{F}}$ *and* $\mathbf{u}_{\mathrm{A}}$ *not both identically zero, satisfying*

$$\int_{\Omega_{\mathrm{F}}} \rho_{\mathrm{F}} c^2 \mathrm{div}\ \mathbf{u}_{\mathrm{F}}\ \mathrm{div}\ \bar{\mathbf{v}}_{\mathrm{F}} + \int_{\Omega_{\mathrm{A}}} K(\omega) \mathrm{div}\ \mathbf{u}_{\mathrm{A}} \mathrm{div}\ \bar{\mathbf{v}}_{\mathrm{A}} = \omega^2 \left( \int_{\Omega_{\mathrm{F}}} \rho_{\mathrm{F}} \mathbf{u}_{\mathrm{F}} \cdot \bar{\mathbf{v}}_{\mathrm{F}} + \int_{\Omega_{\mathrm{A}}} \rho(\omega) \mathbf{u}_{\mathrm{A}} \cdot \bar{\mathbf{v}}_{\mathrm{A}} \right), \tag{80}$$

*for all* $(\mathbf{v}_{\mathrm{F}}, \mathbf{v}_{\mathrm{A}}) \in \mathbf{V}$.

As it is typical in displacement formulations (see [10]), $\omega = 0$ is an eigenfrequency of this problem in both the Darcy's like model and the Allard-Champoux model, with an infinite-dimensional eigenspace given by

$$\mathbf{Z} = \{(\mathbf{u}_{\mathrm{F}}, \mathbf{u}_{\mathrm{A}}) \in \mathbf{V} \ : \ \mathrm{div}\ \mathbf{u}_{\mathrm{F}} = 0 \text{ in } \Omega_{\mathrm{F}}, \ \mathrm{div}\ \mathbf{u}_{\mathrm{A}} = 0 \text{ in } \Omega_{\mathrm{A}} \} \, .$$

This eigenspace consists of pure rotational fluid motions inducing neither variations of pressure in the fluid nor in the porous medium. They are mathematical solutions of the eigenvalue problem with no physical entity because they do not correspond to vibration modes of the coupled system. They arise because no irrotational constraint is imposed to the fluid and porous displacements (see [10]).

# 5 FINITE ELEMENT DISCRETIZATION

Fluid and porous displacements belong to the same class of spaces, $\mathrm{H}(\mathrm{div}, \Omega_{\mathrm{F}})$ and $\mathrm{H}(\mathrm{div}, \Omega_{\mathrm{A}})$, respectively; hence the same type of finite elements should be used for each of them to discretize the variational problem (80).

Let $\mathcal{T}_h$ be a regular tetrahedral partition of $\Omega_{\mathrm{F}} \cup \Omega_{\mathrm{A}}$ such that every tetrahedra is completely contained either in $\Omega_{\mathrm{F}}$ or in $\Omega_{\mathrm{A}}$. We also assume that the faces of tetrahedra lying on $\Gamma_{\mathrm{D}} \cup \Gamma_{\mathrm{N}}$ are completely contained either in $\Gamma_{\mathrm{D}}$ or in $\Gamma_{\mathrm{N}}$.

To approximate the fluid and porous displacements, the lowest order Raviart-Thomas elements (see [27]) are used to avoid spurious modes typical of displacement formulations (see [23]). They consist of vector valued functions which, when restricted to each tetrahedron, are incomplete linear polynomials of the form

$$\mathbf{u}^h(x, y, z) = (a + dx, b + dy, c + dz), \ a, b, c, d \in \mathbb{C}.$$

These vector fields have constant normal components on each of the four faces of a tetrahedron (figure 5) which define a unique polynomial function of this type. Moreover, the global discrete displacement field $\mathbf{u}^h$ is allowed to have discontinuous tangential components on the faces of the tetrahedra of the partition $\mathcal{T}_h$. Instead, its constant normal components must be continuous through these faces (these constant values being the degrees of freedom defining $\mathbf{u}^h$). Because of this, div $\mathbf{u}^h$ is globally well defined in the domain, $\Omega_{\rm F} \cup \Omega_{\rm A}$.

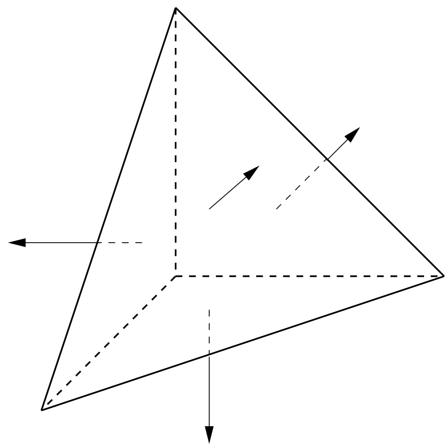

Figure 5: Raviart-Thomas finite element.

Then, for fluid displacements we use the Raviart-Thomas space (see [27])

$$\mathbf{R}_h\left(\Omega_{\rm F}\right) := \{\mathbf{u} \in \mathrm{H}(\mathrm{div}, \Omega_{\rm F}) \;:\; \mathbf{u}|_T \in \mathcal{R}_0(T),\ \forall T \in \mathcal{T}_h,\ T \subset \Omega_{\rm F}\},$$

and an analogous space for porous medium displacements:

$$\mathbf{R}_h\left(\Omega_{\rm A}\right) := \{\mathbf{u} \in \mathrm{H}(\mathrm{div}, \Omega_{\rm A}) \;:\; \mathbf{u}|_T \in \mathcal{R}_0(T),\ \forall T \in \mathcal{T}_h,\ T \subset \Omega_{\rm A}\},$$

where

$$\mathcal{R}_0(T) := \left\{\mathbf{u} \in \mathcal{P}_1(T)^3 \;:\; \mathbf{u}(x,y,z) = (a+dx, b+dy, c+dz),\ a,b,c,d \in \mathbb{C}\right\}.$$

Then, the discrete analogue of $\mathbf{V}$ is

$$\begin{aligned}\mathbf{V}_h := \{(\mathbf{u}_{\rm F}, \mathbf{u}_{\rm A}) \in \mathbf{R}_h\left(\Omega_{\rm F}\right) \times \mathbf{R}_h\left(\Omega_{\rm A}\right) \;:\; \mathbf{u}_{\rm F}\cdot\mathbf{n} = \mathbf{u}_{\rm A}\cdot\mathbf{n} \text{ for each face on } \Gamma_{\rm I},\\ \mathbf{u}_{\rm F}\cdot\boldsymbol{\nu} = 0 \text{ on } \Gamma\cap\partial\Omega_{\rm F},\ \mathbf{u}_{\rm A}\cdot\boldsymbol{\nu} = 0 \text{ on } \Gamma\cap\partial\Omega_{\rm A}\}.\end{aligned}$$

With this finite element space we define an approximate problem to (80):

*Find a complex number $\omega_h$ and a pair of displacements $(\mathbf{u}_{\rm F}^h, \mathbf{u}_{\rm A}^h) \in \mathbf{V}_h$ not both identically zero, such that*

$$\int_{\Omega_{\rm F}} \rho_{\rm F} c^2 \mathrm{div}\ \mathbf{u}_{\rm F}^h\ \mathrm{div}\ \bar{\mathbf{v}}_{\rm F}^h + \int_{\Omega_{\rm A}} K(\omega_h)\mathrm{div}\ \mathbf{u}_{\rm A}^h\ \mathrm{div}\ \bar{\mathbf{v}}_A^h = \omega_h^2\left(\int_{\Omega_{\rm F}} \rho_{\rm F}\mathbf{u}_{\rm F}^h\cdot\bar{\mathbf{v}}_{\rm F}^h + \int_{\Omega_{\rm A}} \rho(\omega_h)\mathbf{u}_{\rm A}^h\cdot\bar{\mathbf{v}}_{\rm A}^h\right), \quad (81)$$

*for all $(\mathbf{v}_{\rm F}^h, \mathbf{v}_{\rm A}^h) \in \mathbf{V}_h$.*

# 6 MATRICIAL DESCRIPTION

In the previous section, a discrete formulation of our eigenvalue problem has been stated. Now a matricial description is given and it is shown that it is a well posed symmetric nonlinear generalized eigenvalue problem involving sparse matrices.

Let $u_{\rm F}^h$ and $v_{\rm F}^h$ denote the column vectors of components of $\mathbf{u}_{\rm F}^h$ and $\mathbf{v}_{\rm F}^h$, respectively, in the standard finite element basis associated with $\mathbf{R}_h(\Omega_{\rm F})$. Similarly, let $u_{\rm A}^h$ and $v_{\rm A}^h$ denote the column vectors of components of $\mathbf{u}_{\rm A}^h$ and $\mathbf{v}_{\rm A}^h$, respectively, in the standard finite element basis associated with $\mathbf{R}_h(\Omega_{\rm A})$. Then the problem (81) can be written in matrix form as

$$\begin{pmatrix} R_{\rm F} & 0 \\ 0 & R_{\rm A}(\omega_h) \end{pmatrix} \begin{pmatrix} u_{\rm F}^h \\ u_{\rm A}^h \end{pmatrix} = \omega_h^2 \begin{pmatrix} M_{\rm F} & 0 \\ 0 & M_{\rm A}(\omega_h) \end{pmatrix} \begin{pmatrix} u_{\rm F}^h \\ u_{\rm A}^h \end{pmatrix}, \tag{82}$$

where

$$\begin{aligned} {v_{\rm F}^h}^* R_{\rm F} u_{\rm F}^h &= \int_{\Omega_{\rm F}} \rho_{\rm F} c^2 \operatorname{div} \mathbf{u}_{\rm F}^h \operatorname{div} \bar{\mathbf{v}}_{\rm F}^h, && (83)\\ {v_{\rm A}^h}^* R_{\rm A}(\omega_h) u_{\rm A}^h &= \int_{\Omega_{\rm A}} K(\omega_h) \operatorname{div} \mathbf{u}_{\rm A}^h \operatorname{div} \bar{\mathbf{v}}_{A}^h, && (84)\\ {v_{\rm F}^h}^* M_{\rm F} u_{\rm F}^h &= \int_{\Omega_{\rm F}} \rho_{\rm F} \mathbf{u}_{\rm F}^h \cdot \bar{\mathbf{v}}_{\rm F}^h, && (85)\\ {v_{\rm A}^h}^* M_{\rm A}(\omega_h) u_{\rm A}^h &= \int_{\Omega_{\rm A}} \rho(\omega_h) \mathbf{u}_{\rm A}^h \cdot \bar{\mathbf{v}}_{\rm A}^h. && (86) \end{aligned}$$

$R_{\rm F}$ and $M_{\rm F}$ are the standard stiffness and mass matrices of the fluid, respectively, while $R_{\rm A}(\omega_h)$ and $M_{\rm A}(\omega_h)$ are the corresponding ones for the porous medium. Notice that every matrix is highly sparse because only a maximum of seven entries per row can be different from zero (this corresponds to the number of faces of two adjacent tetrahedra).

Both matrices in the eigenvalue problem (82) are singular; however, by performing a translation in the eigenvalues, it can be written in an equivalent more convenient way:

$$\begin{pmatrix} R_{\rm F} + M_{\rm F} & 0 \\ 0 & R_{\rm A}(\omega_h) + M_{\rm A}(\omega_h) \end{pmatrix} \begin{pmatrix} u_{\rm F}^h \\ u_{\rm A}^h \end{pmatrix} = (\omega_h^2 + 1) \begin{pmatrix} M_{\rm F} & 0 \\ 0 & M_{\rm A}(\omega_h) \end{pmatrix} \begin{pmatrix} u_{\rm F}^h \\ u_{\rm A}^h \end{pmatrix}. \tag{87}$$

Now, matrix $R_{\rm F} + M_{\rm F}$ is clearly positive definite, hence non-singular and symmetric. However, the matrix $R_{\rm A}(\omega_h) + M_{\rm A}(\omega_h)$ is singular if there exists $\omega_h$ such that $\rho(\omega_h)$ or $K(\omega_h)$ are null. When we use the Darcy's like model, the dynamic density is null only if $\omega_h = i\frac{\sigma}{\rho_{\rm F}}$ (which is an eigenvalue associated to null divergence displacements in the porous medium) while the bulk modulus is positive. In the case of Allard-Champoux model, there exists a frequency $\omega_h$ such that $K(\omega_h)$ is null but this is not true for $\rho(\omega_h)$.

Thus, except for this special case, the matrix on the left hand side is non-singular and, consequently, it can be used to build a well posed generalized eigenvalue problem to help us to solve the non-linear eigenvalue problem (82). With this aim, we can define a function $S : \mathbb{C} \to \mathbb{C}$ such that $S(\omega_h) = \lambda_h$, where $\lambda_h$ is the least modulus eigenvalue of the following problem,

$$\begin{pmatrix} R_{\rm F} + M_{\rm F} & 0 \\ 0 & R_{\rm A}(\omega_h) + M_{\rm A}(\omega_h) \end{pmatrix} \begin{pmatrix} u_{\rm F}^h \\ u_{\rm A}^h \end{pmatrix} = \lambda_h \begin{pmatrix} M_{\rm F} & 0 \\ 0 & M_{\rm A}(\omega_h) \end{pmatrix} \begin{pmatrix} u_{\rm F}^h \\ u_{\rm A}^h \end{pmatrix}. \tag{88}$$

The function $S$ is well defined because the generalized eigenvalue problem is well posed. Furthermore, both matrices of this problem are symmetric and highly sparse and, hence, convenient for computational purposes. Finally, calculation of the eigenvalues of the problem (82) is equivalent to find the roots $\omega_h$ of the nonlinear equation,

$$S(\omega_h) - (\omega_h^2 + 1) = 0. \tag{89}$$

A similar problem arising from finite element analysis of dissipative acoustic models can be found in [9].

# 7 NUMERICAL RESULTS

In this section we present some numerical results obtained with a computer code implementing the numerical method given in this paper. This code allows us to compute the response diagram of enclosures as those in figures 1 and 2, consisting of several layers of fluids and porous media, and also to solve the nonlinear eigenvalue problem (80) by means of a secant method combined with an inverse power method. This type of method has been already used in other works devoted to solve nonlinear eigenvalues problems (see [9]).

In order to validate our method, we have considered the following data: fluid is air with density $\rho_{\mathrm{F}} = 1.225$ kg/m$^3$, $c = 343$ m/s whereas properties of the porous material are summarized in $\sigma = 10^4$ kg/(m$^3$s), $\phi = 0.71$, $\gamma = 1.4$, $N_{pr} = 0.702$ and $P_0 = 101320$ Pa. Concerning dimensions of enclosures shown in figures 1 and 2, they are as follows: length and width are 4 m whereas height is 2 m for the first layer of free fluid, 0.05 m for the second layer of porous material and 0.1 m for the third layer of free fluid in the case of the enclosure in figure 1.

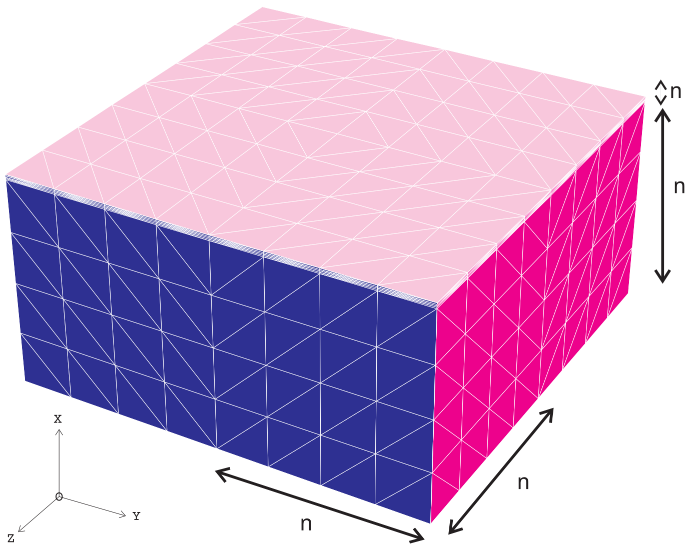


Figure 6: Mesh 2 corresponding to the enclosure shown in figure 2

These two enclosures have been decomposed in tetrahedra (see figure 6). Depending on which one is considered and on the degree of mesh refinement (parameter $n$ refers to the number of divisions introduced for each layer of the enclosure in figure 6), the meshes are denoted as it is shown in table 1.

| | Mesh 0 | Mesh 1 | Mesh 2 | Mesh 3 | Mesh 4 |
|---|---|---|---|---|---|
| Sample | Figure 1 | Figure 1 | Figure 2 | Figure 2 | Figure 2 |
| n | 2 | 4 | 6 | 8 | 10 |
| Degrees of freedom | 1072 | 8128 | 21600 | 50688 | 98400 |

Table 1: Name and degrees of freedom for the different meshes.

| Mode | Mesh 2 | Mesh 3 | Mesh 4 | Extrapolated | Exact |
|---|---|---|---|---|---|
| $\omega^F_{100}$ | 265.791+0.382 i | 265.891+0.287 i | 265.961+0.242 i | 266.708+0.162 i | 266.026+0.164 i |
| $\omega^F_{110}$ | 375.722+0.786 i | 375.894+0.593 i | 375.977+0.502 i | 376.144+0.338 i | 376.132+0.342 i |
| $\omega^F_{001}$ | 523.913+1.943 i | 524.685+1.284 i | 525.038+0.965 i | 525.644+0.332 i | 525.656+0.389 i |
| $\omega^F_{200}$ | 531.251+1.704 i | 531.418+1.284 i | 531.506+1.087 i | 531.733+0.772 i | 531.680+0.737 i |
| $\omega^F_{020}$ | 528.894+1.684 i | 530.052+1.273 i | 530.622+1.081 i | 531.807+0.730 i | 531.680+0.737 i |

Table 2: Rigid porous medium and air. Darcy's like model.

Firstly we consider the enclosure in figure 2. In table 2 we show the first complex eigenfrequencies (in Hz) for three different meshes: mesh 2, mesh 3 and mesh 4. One could see that they have a small imaginary part and a real part "close" to the response peaks. We also include the extrapolated complex eigenfrequencies computed by the least square method, and the exact ones corresponding to both Darcy's like model and Allard-Champoux model, obtained by solving their respective nonlinear system of equations, for any pair of integers $j$ and $k$, namely,

$$\mu_{\mathrm{F}}^2 + \frac{\omega^2}{c^2} = \frac{\pi^2}{b^2} j^2 + \frac{\pi^2}{d^2} k^2, \tag{90}$$

$$\mu_{\mathrm{A}}^2 + \frac{\omega^2 \rho(\omega)}{K(\omega)} = \frac{\pi^2}{b^2} j^2 + \frac{\pi^2}{d^2} k^2, \tag{91}$$

$$\mu_{\mathrm{F}} \rho(\omega) \cosh(a_{\mathrm{A}} \mu_{\mathrm{A}}) \sinh(a_{\mathrm{F}} \mu_{\mathrm{F}}) = -\mu_{\mathrm{A}} \rho_{\mathrm{F}} \sinh(a_{\mathrm{A}} \mu_{\mathrm{A}}) \cosh(a_{\mathrm{F}} \mu_{\mathrm{F}}). \tag{92}$$

An excellent agreement can be observed between exact and computed values, even for the coarser mesh. This shows the effectiveness of the method. From this table we have calculated the order of convergence of the method and found that it is approximately $O(h^2)$, $h$ being a parameter associated with the mesh size, which is optimal for the lowest order Raviart-Thomas finite elements we have used.

| Mode | Mesh 2 | Mesh 3 | Mesh 4 | Extrapolated | Exact |
|---|---|---|---|---|---|
| $\omega_{00}^F$ | 8163.265 i | 8163.265 i | 8163.265 i | 8163.265 i | 8163.265 i |
| $\omega_{10}^F$ | 8156.630 i | 8157.003 i | 8157.277 i | 8163.163 i | 8158.435 i |
| $\omega_{11}^F$ | 8149.990 i | 8150.735 i | 8151.285 i | 8163.382 i | 8153.605 i |

Table 3: Rigid porous medium and air. Darcy's like model. Overdamped modes.

On the other hand, according to the analysis in section 3, there exist overdamped modes. In spite of the fact that these overdamped modes are not the magnitudes of interest, from the numerical point of view it is important to know if they are well approximated by the finite element method. Otherwise they could be a source of spectral pollution. Table 3 includes the computed and exact purely imaginary eigenfrequencies of higher modulus for the same three meshes described above.

When the Allard-Champoux model is used we obtain similar results to those previously obtained for the Darcy's like model. They are shown in tables 4 and 5.

| Mode | Mesh 2 | Mesh 3 | Mesh 4 | Extrapolated | Exact |
|---|---|---|---|---|---|
| $\omega_{100}^F$ | 264.498+0.768 i | 264.545+0.582 i | 264.570+0.495 i | 264.641+0.336 i | 264.622+0.340 i |
| $\omega_{110}^F$ | 373.830+1.586 i | 373.915+1.212 i | 373.968+1.033 i | 374.195+0.692 i | 374.082+0.712 i |
| $\omega_{001}^F$ | 519.622+4.457 i | 519.968+3.274 i | 520.166+2.687 i | 520.829+1.440 i | 520.584+1.606 i |
| $\omega_{200}^F$ | 528.662+3.436 i | 528.559+2.652 i | 528.550+2.266 i | 528.535+1.461 i | 528.598+1.561 i |
| $\omega_{020}^F$ | 526.277+3.395 i | 527.194+2.630 i | 527.670+2.254 i | 528.816+1.475 i | 528.598+1.561 i |

Table 4: Rigid porous medium and air. Allard-Champoux model.

| Mode | Mesh 2 | Mesh 3 | Mesh 4 | Exact |
|---|---|---|---|---|
| $\omega_{100}^F$ | 4983.698 i | 4439.175 i | 4439.603 i | 4438.380 i |
| $\omega_{110}^F$ | 4979.907 i | | 4436.174 i | 4436.828 i |
| $\omega_{001}^F$ | 4976.004 i | 4435.718 i | 4435.633 i | 4435.279 i |

Table 5: Rigid porous medium and air. Allard-Champoux model. Overdamped modes.

Nevertheless, when calculating overdamped modes with the Allard-Champoux model some difficulties appear due to the highly oscillating eigenfunction associated with it. This means that a very refined mesh might be used in order to get a suitable approximation. In fact, only with mesh 4 good accuracy has been achieved. Figure 7 shows the oscillation in the eigenvector in a plane near the interface between the fluid and the porous material.

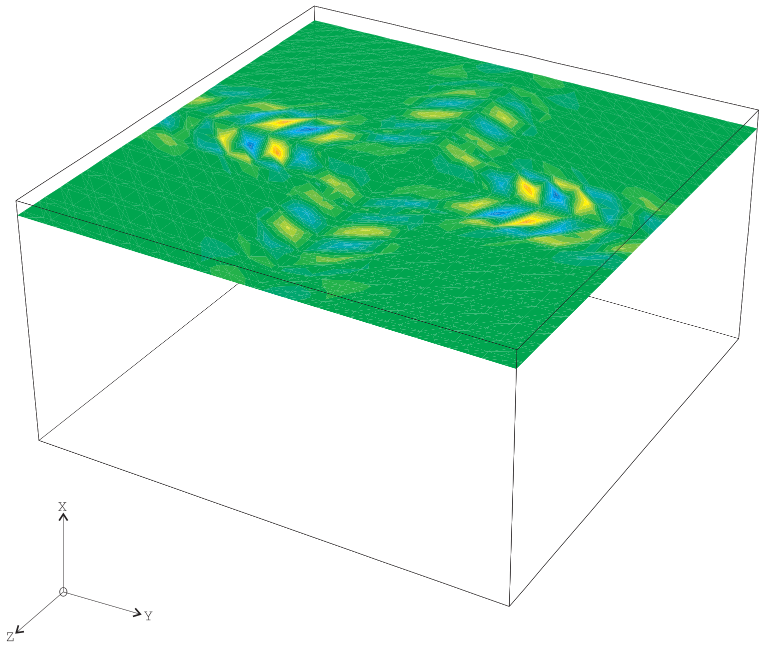


Figure 7: Eigenvector for an overdamped mode with Allard-Champoux model

Finally, we consider the enclosure shown in figure 1. The response curves are drawn in figure 8 when the model is solved with mesh 0 and mesh 1. In these curves $\log_{10} ||p||_{\mathrm{L}^2}$ is plotted for angular frequencies $\omega$ ranging from 50 to 1000 Hz.

Several response peaks can be observed in these curves depending on the refinement of the mesh. We notice that the finer the mesh, the smaller the number of peaks in the response diagram. Moreover, table 6 shows the computed (complex) resonance frequencies for the damped coupled system shown in figure 1 and the (real) eigenfrequencies of a similar undamped enclosure where the porous material has been replaced with air. As one can see, all are quite similar.

| Undamped peaks | Complex eigenfrequencies | Damped peaks Mesh 0 | Damped peaks Mesh 1 |
|---|---|---|---|
| 269.392 | 266.189+1.495 i | 250.5 | 250.5 |
| 588.840 | 594.737+8.535 i | 572.5 | 581.0 |
| 751.297 | 751.811+1.506 i | 720.5 | 748.0 |
| 808.175 | 797.242+1.750 i | 785.5 | - |
| 924.519 | 936.395+5.309 i | 921.0 | - |

Table 6: Resonance vibration frequencies and complex eigenfrequencies

# 8 CONCLUSIONS

In this paper a three-dimensional finite element method has been implemented to solve the system of equations modelling the macroscopic behavior of a porous material with rigid solid frame. It allows us to compute both the response to an harmonic excitation and the free vibrations of a three-dimensional multilayer system consisting of different layers composed of free fluids and rigid porous media. The finite element used is the lowest order face element introduced by Raviart and Thomas, with the advantage of eliminating the spurious modes.

For rigid porous media we have considered two models: a Darcy's like model and the Allard-Champoux model. These two models are equivalent when frequency is much lower than resistivity.

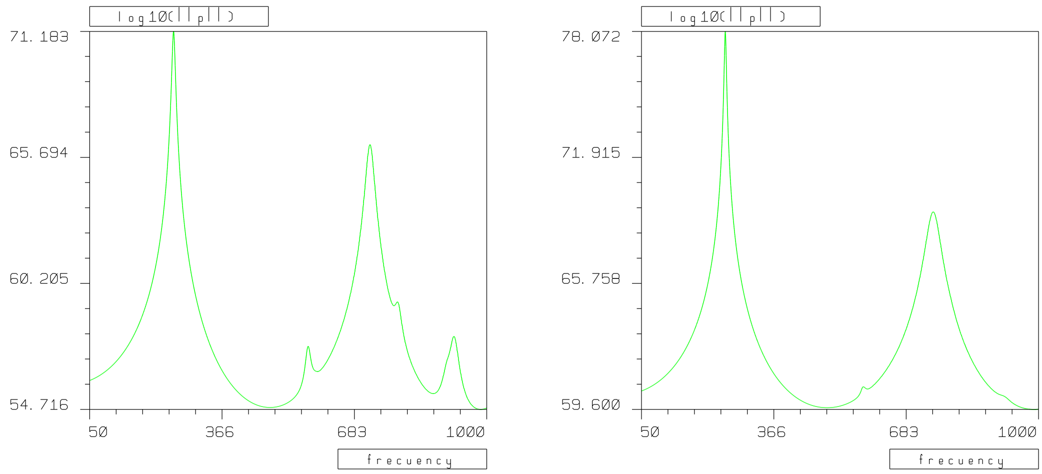


Figure 8: Response curve with Mesh 0 and Mesh 1

When solving the problem of free vibrations, the computer program predicts very well the exact complex eigenfrequencies for the Darcy's like model in the case of a test example. This is true even for the overdamped modes. On the other hand, when using the Allard-Champoux model, the eigenfrequencies with non-null real part are well approximated whereas calculation of overdamped modes is much more complicated due to the highly oscillating eigenfunction associated with them, as observed in figure 7. This forces us to use very fine meshes.

# References


[1] J.-F. Allard. *Propagation of sound in porous media: modelling sound absorbing materials*, Elsevier, New York, 1993.

[2] J.-F. Allard, A. Aknine, C. Depollier. *Acoustical properties of partially reticulated foams with high and medium flow resistance*, J. Acoust. Soc. Am. **79** (1986), 1734-1740.

[3] J.-F. Allard, Y. Champoux. *New empirical equations for sound propagation in rigid frame fibrous materials*, J. Acoust. Soc. Am. **91** (6) (1992), 3346-3353.

[4] J.-F. Allard, C. Depollier, J. Nicolas, W. Lauriks, A. Cops. *Propriétés acoustiques des matériaux poreux saturés d'air et théorie de Biot*, J. Acoust. **3** (1990), 29-38.

[5] N. Atalla, R. Panneton, P. Debergue. *A mixed displacement pressure formulation for poroelastic materials*, J. Acoust. Soc. Am. **104** (1998), 1444-1452.

[6] K. Attenborough. *Acoustical characteristics of rigid fibrous absorbents and granular materials*, J. Acoust. Soc. Am. **73** (1983), 785-799.

[7] A. Bermúdez, J.L. Ferrín, A. Prieto. *Finite element solution of new displacement/pressure poroelastic models in acoustics*, Submitted for publication to Comput. Methods Appl. Mech. Eng.

[8] A. Bermúdez, L. Hervella, R. Rodríguez. *Finite element computation of three-dimensional elastoacoustic vibrations*, J. Sound Vib. **219** (2) (1999), 279-306.

[9] A. Bermúdez, L. Hervella, R. Rodríguez. *Finite element computation of the vibrations of a plate-fluid system with interface damping*, Comput. Methods Appl. Mech. Engrg. **190** (2001), 3021-3038.

[10] A. Bermúdez, R. Durán, M.A. Muschietti, R. Rodríguez, J. Solomin. *Finite element vibration analysis of fluid-solid systems without spurious modes*, SIAM J. Numer. Anal. **32** (1995), 1280-1295.

[11] M.A. Biot. *Theory of propagation of elastic waves in a fluid-saturated porous solid. I. Lower frequency range*, and *II. Higher frequency range*, J. Acoust Soc. Am. **28** (2) (1956), 168-178 and 179-191.

[12] M.A. Biot. *Generalized theory of acoustic propagation in porous dissipative media*, Jour. Acoustic Soc. Amer. **34** (1962), 1254-1264.

[13] Y. Champoux, J.-F. Allard. *Dynamic tortuosity and bulk modulus in air-saturated porous media*, J. Appl. Phys. **70** (1991), 1975-1979.

[14] Y. Champoux, M.R. Stinson. *On acoustical models for sound propagation in rigid frame porous materials and the influence of shape factors*, J. Acoust. Soc. Am. **92** (2) (1992), 1120-1131.

[15] Th. Clopeau, J.L. Ferrín, R.P. Gilbert, and A. Mikelić. Homogenizing the acoustic properties of the seabed. Part II. *Math. Comput. Modelling*, **33** (8-9) (2001), 821-841.

[16] M.A. Delany, E.N. Bazley. *Acoustic properties of fibrous absorbent materials*, Appl. Acoust. **3** (1970), 105-116.

[17] V. Easwaran, W. Lauriks, J.P. Coyette. *Displacement-based finite element method for guided wave propagation problems: application to poroelastic media*, J. Acoust. Soc. Am. **100** (5) (1996), 2989-3002.

[18] H.I. Ene, E. Sanchez-Palencia. *Equations et phénomenènes de surface pour l'écoulement dans un modèle de milieu poreux*, J. Mécan. **14** (1975), 73-108.

[19] J.L. Ferrín and A. Mikelić. Homogenizing the acoustic properties of a porous matrix containing an incompressible inviscid fluid. *Math. Methods Appl. Sci.*, **26** (10) (2003), 831-859.

[20] R.P. Gilbert and A. Mikelić. Homogenizing the acoustic properties of the seabed. Part I. *Nonlinear Anal.*, **40** (1-8) (2000), 185-212.

[21] P.Göransson. *A 3-D, simmetric, finite element formulation of the Biot equations with application to acoustic wave propagation through an elastic porous medium*, Int. J. Numer. Meth. Engng., **41** (1998), 167-192.

[22] D.L. Johnson, J. Koplik, R. Dashen. *Theory of dynamic permeability and tortuosity in fluid saturated porous media*, J. Fluid Mech, **176** (1987), 379-402.

[23] L. Kiefling, G.C. Feng. *Fluid-structure finite element vibration analysis*, AIAA J. **14**, (1977), 292-315.

[24] A. Mikelić. *Homogenization theory and applications to filtration through porous media*, Lecture Notes in Mathematics 1734, Springer, (2000), 127-214.

[25] P.M. Morse, K.U. Ingard. *Theoretical acoustics*, McGraw-Hill, New York, 1978.

[26] R. Panneton, N. Atalla. *An efficient finite element scheme for solving the three-dimensional poroelasticity problem in acoustics*, J. Acoust. Soc. Am. **101** (6) (1997), 3287-3298.

[27] P.A. Raviart, J.M Thomas. *A mixed finite element method for second order elliptic problems*, in Mathematical Aspects of Finite Element Methods, Lecture notes in Mathematics 606, Springer Verlag, (1977), 292-315.

[28] E. Sanchez-Palencia. *Non-homegeneous media and vibration theory*, Lecture Notes in Physics 127, Springer Verlag, 1980.

[29] N.-M. Shiau. *Multi-dimensional wave propagation in elastic porous materials*, Ph.D. thesis, School of Mechanical Engineering, Purdue University, 1991.

[30] C. Zwikker, C.W. Kosten. *Sound absorbing materials*, Elsevier, New York, 1949.